

Biosynthesis of Silver Nanoparticles by Using Green Tea (*Camellia sinensis*) Extracts

Hawazen H. Salih  

Department of Genetic Engineering., Genetic Engineering and Biotechnology Institute for post graduate studies, University of Baghdad, Baghdad, Iraq

Received 08/01/2023, Revised 29/05/2023, Accepted 31/05/2023, Published Online First 20/10/2023, Published 01/05/2024



© 2022 The Author(s). Published by College of Science for Women, University of Baghdad.

This is an Open Access article distributed under the terms of the [Creative Commons Attribution 4.0 International License](https://creativecommons.org/licenses/by/4.0/), which permits unrestricted use, distribution, and reproduction in any medium, provided the original work is properly cited.

Abstract

Due to its availability, affordability, effectiveness, and low cost, the green-based synthesis of silver nanoparticles by plants is gaining popularity. It is safe to handle and has a wide range of metabolites, including antioxidant and antibacterial activities. The production of AgNPs was established in this work utilizing aqueous and methanolic extracts of fresh *Camellia sinensis* leaves that reduced silver nitrate. This process enabled the creation of NPs, which were then characterized using a range of analytical techniques including ultraviolet-visible (UV-Vis) spectrophotometry, Fourier Transform Infrared spectroscopy (FTIR), Atomic Fluorescence Microscopy (AFM), X-ray scattering (XRD), and Zeta potential analyzer. The color of aqueous silver nitrate changes following treatment with fresh leaf extracts, and was confirmed by UV-Vis spectra. In addition, the AFM analysis that showed particles were spherical, either individually or together with average sizes 108.3 and 84.76 nm for aqueous and methanolic extracts respectively. The crystalline nature of the nanoparticles was verified by the XRD method. The average size was estimated according to the Scherrer equation and they were 61.24, 99.66 nm for *Camellia sinensis* silver nanoparticles (CANPs) aqueous and methanolic extracts respectively. In addition the zeta potential values were -30.31 and -32.33 mV for CANPs aqueous and methanolic extracts respectively.

Keywords: AFM, *Camellia sinensis*, FTIR, Silver nanoparticles, UV, XRD, Zeta potential analyzer.

Introduction

The study of science, engineering, and technology at the nanoscale, or between 1 and 100 nm, is known as nanotechnology. This cutting-edge technology is employed in a variety of areas, including chemistry, materials science, and others of the same kind. Additionally, numerous varieties of nanoparticles are applied in medicine as imaging agents or medication carriers. Different produced liposome nanoparticles kinds are now employed as vaccination and anti-cancer medication delivery

systems. Additionally, gold nanoparticles are utilized in home pregnancy test kits ^{1,2}.

Chemical procedures are recognized to be riskier than green synthesis. This is so that the latter can produce nanoparticles in a manner that is acknowledged as being more environmentally benign and sustainable (NPs) ³. Some of the unique green methodologies, such as emerging green nanotechnology, have shown to be crucial in the

production of newer nanoparticles. These alternate approaches, which have shown to be more successful in producing NPs are those that incorporate microbes and plant extracts ⁴.

Although there are many metals in nature, they are manufactured on a large scale by using a few of them such as gold, silver, palladium and platinum in the form of nanostructures ⁵, among the above meta metals, silver nanoparticles have attracted much attention due to their unique properties for use in various applications including pharmacology, agriculture, water detoxification, air purification, textile industries and as a catalyst in oxidation

Materials and Methods

Collection of *Camellia sinensis* L.

Camellia sinensis were obtained from the plantation in Baghdad city, identification as (*Camellia sinensis* L.) by a professional in the Biology Department/College of Science/University of Baghdad. To obtain *Camellia sinensis* extract the plant were leaves cleansed and lichens scraped away before drying in the shade on clean drying tables. The plant components were then cut with a knife into smaller pieces and pulverized using an electric laboratory grinder into powder form. Firstly, in order to remove the oil from the leaves, 200 grams of *Camellia sinensis* leaves powder was macerated with 1 liter of petroleum ether solvent. The residue was collected, air-dried and separated into two batches. Each batch of the defatted plant leaves was individually extracted with water and methanol to prepare aqueous and methanolic extracts. In two separate extraction bottles, 200 g of each powdered plant material was dissolved in 1 liter of sterile distilled de-ionized water and 1 liter (L) of methanol alcohol, and allowed to stand for five days in the dark with occasional daily stirring for homogeneous mixing and extraction. After the crude extract was sieved, the filtrate was concentrated by evaporating over steel pans in a 37°C oven. Evaporation is followed by transfer to tubes, where it is then kept in a refrigerator at 4°C ¹².

Preparation of green silver nanoparticles using *Camellia sinensis* extracts

Preparation of green silver nanoparticles by *Camellia sinensis* aqueous and methanolic extracts

reactions ⁶. In addition, the important properties of its antibacterial activity against a wide range of bacteria without any toxicity to animal cells ⁷.

Currently, silver nanoparticles are utilized as antiseptics, antibiotics, dental materials; burn wound treatments, and catheters to inhibit the development of germs in a number of applications^{8,9}. Aside from that, biological elements like bacteria, fungi, and algae, as well as their enzymes, may be employed to alter the physical, mechanical, and structural properties of AgNPs of various sizes and shapes ^{10,11}.

were done according to Ojha *et al.* ¹³ and Krishnadhas *et al.* ¹⁴ with some modifications. In 95 ml of a 10 mM silver nitrate AgNO₃ solution, 5 ml of each extract was sprayed dropwise, separately (made by dissolving 1.69 g AgNO₃ into 1 L deionized water) under ultrasonic conditions, with an ultrasonic power of 100 W and a frequency of 42 kHz. After 20 minutes of sonication, the solutions were stored at 25°C in opaque bottles. After being stirred at 800 rpm for 30 minutes, After 24 hours, the reaction mixture was centrifuged for 10 minutes at 10,000 rpm to separate the clear supernatant.

The last colloid samples were stored in a refrigerator at 4°C in opaque vials. Over a period of five days, the color of *Camellia sinensis* silver nanoparticles (CAgNPs) solutions altered, demonstrating the production of silver nanoparticles (AgNPs).

Characterization of the prepared nanoparticles

Characterization measurements (morphological and structural) of silver nanoparticles for identifying AgNPs in this study, were implemented by many different techniques, as follows:

UV-Visible Absorption Spectroscopy

UV-Visible spectroscopy provides that the silver ions in the colloidal solution had been reduced. With pure water used as a reference, a tiny aliquot of AgNPs was placed in a quartz cuvette and monitored for wavelength scanning between 200 and 800 nm.

After adding green tea extract to an AgNO₃ solution, the UV-Vis absorption spectra of the sample were measured using a Perkin Elmer Spectrophotometer at various times of 5, 10, 15, and 20 minutes¹⁵.

Fourier Transform Infrared (FTIR) Spectroscopy Analysis

FTIR analysis (Shimadzu) was used to study the characterization of functional groups on the AgNPs by plant extracts, and the spectra were scanned in the 4000-400 cm⁻¹ range at a resolution of 4 cm⁻¹. The samples were produced by spreading them on a glass slide in accordance with the accepted practices. The sample was then looked at after that¹⁶.

Atomic force microscopy

One of the first methods for seeing, measuring, and modifying materials at the nanoscale is atomic force microscopy (AFM). It offers the capacity to see 3D objects as well as qualitative and quantitative data on a variety of physical characteristics, such as size, morphology, surface texture, and roughness¹⁷. Each type of nanoparticle sample was applied as a thin layer on a glass slide using 100 µl of the sample, which was then let to dry for five minutes. The slides were then scanned using the AFM¹⁸.

X-ray diffractometer

The analysis using an X-ray diffractometer (XRD) is useful for knowing the phase structure and

purity of synthesized green AgNPs and is generally used as a common technique to study the crystal structure and phase composition of AgNPs. On a glass slide, a thin layer of homogeneous water hung from each type of nanoparticle was created and allowed to dry. The X-ray diffraction (XRD) pattern (operating voltage 40 kV and current 30 mA, Cu K (α) radiation ($\lambda = 1.540$) was captured using an X-ray diffractometer¹³. Data were collected for the 2θ range of 10 to 80 degrees with a 0.0200 degree step. The result of the XRD pattern was interpreted using the reference standard for describing AgNPs developed by the Joint Committee on Powder Diffraction Standards (JCPDS card number 04-0783). The Debye-Scherrer equation was used to determine the particle size of the generated samples, and it is as follows:

$$D=0.9 \lambda/B \cos\Theta$$

In this equation, D stands for the size of the crystal, λ is the x-ray wavelength, the diffraction angle (Braggs angle) in radians, and β is the entire width at half maximum of the peak in radians¹⁹.

Zeta potential analyzer

The produced nanoparticles' stability was assessed using a zeta potential analyzer that can function between -160 mV and +160 mV, and the findings were shown in graph²⁰.

Results and Discussion

Biosynthesis and characterization of nanoparticles

Methanolic and aqueous extracts of *Camellia sinensis* were used to make the silver nanoparticles. Compared to other bio reductants, the production of metallic nanoparticles utilizing plant extracts is easier and more successful²¹. It is widely known that phytochemicals not only convert Ag⁺ into Ag⁰ but also cap the Ag⁺ to create these very stable nanoparticles^{22,23}. In this study, the formation of silver nanoparticles was monitored depending on color change and UV spectroscopy absorption. The colors of the green silver nanoparticle solutions were changed for *Camellia sinensis* silver nanoparticles (CAGNPs) from dark green to light brownish green,

with the addition of *Camellia sinensis* methanolic and aqueous extracts, respectively, to silver nitrate solution. The color began to change after 24 hours, and after 48 hours the color changed to the final color. The presence of active molecules in the methanolic and aqueous extracts of *Camellia sinensis* implies the synthesis of silver nanoparticles (AgNPs) by the reduction of silver metal ions Ag⁺ into silver nanoparticles Ag⁰. The stability and transformation of metallic silver into AgNPs depend on compounds including phenols, terpenoids, alkaloids, flavonoids, proteins, and carbohydrates¹³. By lengthening the incubation period, it is possible to further accelerate the rate of particle formation and decrease it, which causes the color's intensity to rise

as the reaction time increases²⁴. Due to their optical characteristics, metal nanoparticles exhibit a range of hues in solutions²⁵. The activation of the metal nanoparticles' surface plasmon resonance is what causes the color shift (SPR). Silver nanoparticles' fascinating optical properties are directly tied to localized surface plasmon resonance, which is greatly influenced by the form of the nanoparticles²⁶. This outcome is in agreement with Saliem *et al.*²⁴ and Thamer²⁷, who demonstrated the possibility of color change following the reduction of silver ions into silver nanoparticles following contact with plant extracts. As a result, AgNP characterization is crucial for assessing the functional properties of the produced particles. Other researchers had also chosen *Camellia sinensis* leaf extract as a reducing biomaterial^{12,15}

UV-Visible spectroscopy

UV-Vis spectroscopy is one of the primary techniques for identifying and quantifying the production of NPs. UV-Vis spectroscopy was utilized to confirm the stability of the synthesized AgNPs since the plasmon band of Ag is sensitive to the size and shape of the generated NPs²⁸. The elements in the plant extract cause the silver ions to be reduced to silver atoms²⁹.

UV-visible spectroscopy is an important step in confirming the synthesis of AgNPs and the color

change. When the *Camellia sinensis* extract was mixed with an aqueous solution of AgNO₃, this resulted in a change of color. This change in color is a result of the collective oscillation of free electrons of silver nanoparticles in resonance with the light wave in silver nanoparticle synthesis and this oscillation gives a typical peak value. UV-visible spectra of the plant extracts without AgNO₃ solution and with it were shown in Fig. 1 and 2. The existence of many chemical compounds known to interact with silver ions is indicated by the faint absorption peak at 200 nm²⁶. The type, size, and morphologies of the NPs generated, the dielectric constant of the medium and temperature, as well as their interparticle distances, all have a remarkable impact on the surface plasmon resonance absorbance^{30, 31}. The absorption spectrum was recorded between 200 nm and 800 nm. It is observed that the silver surface plasmon resonance band centered at 263 nm in the (CAgNPs) aqueous extract and 270 nm in the methanolic (CAgNPs) extract, in comparison with UV Test for *Camellia sinensis* methanolic and aqueous extract 271 and 272 nm respectively.

AgNPs made via biological processes were monitored for more than a year for stability, and an SPR peak at the same wavelength was seen using UV-vis spectroscopy³².

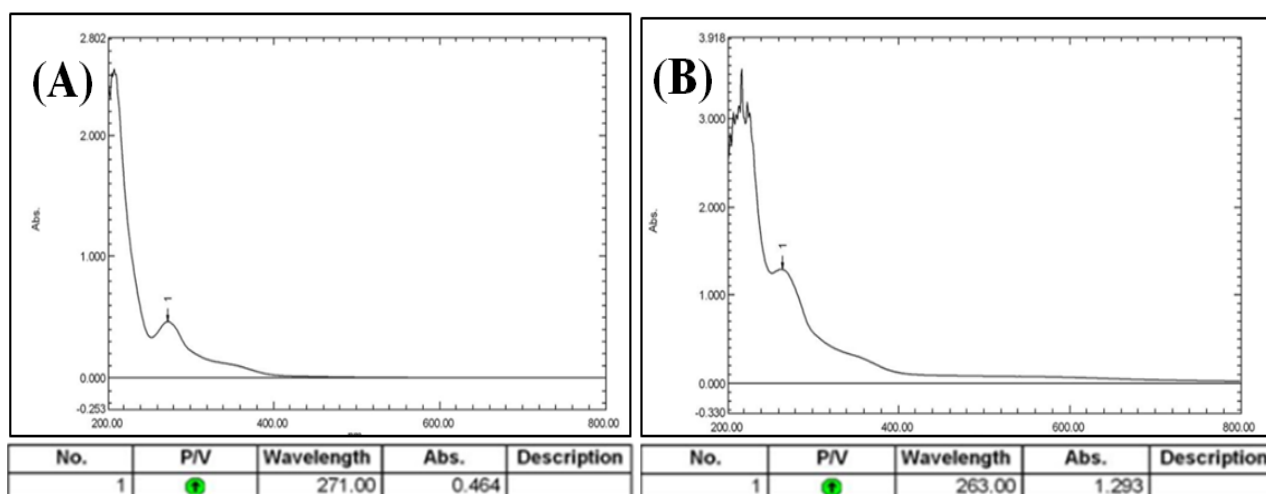


Figure 1. UV-Visible spectral analysis of (A): *Camellia sinensis* aqueous extract, (B): synthesized (CAgNPs) aqueous extract

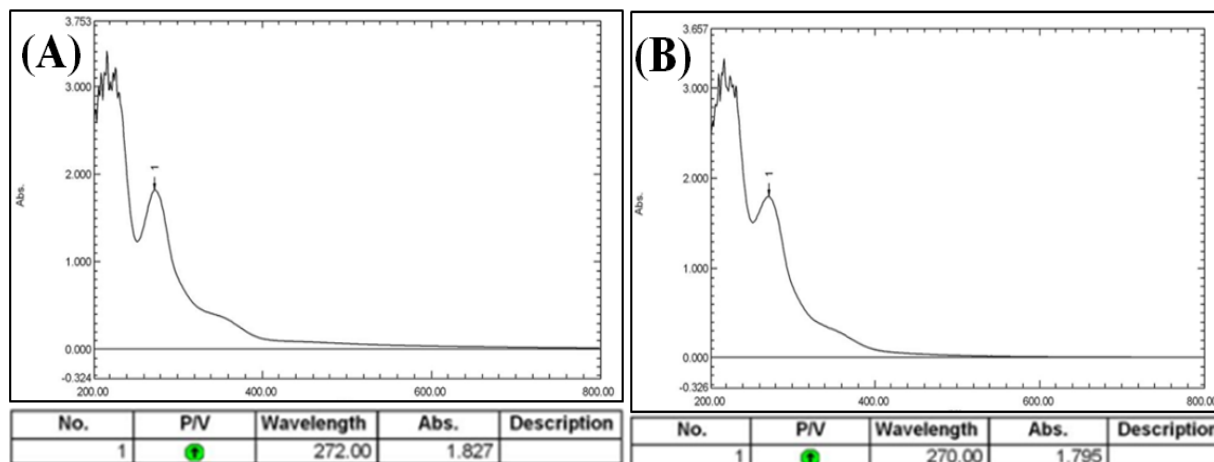


Figure 2. UV-Visible spectral analysis of (A): *Camellia sinensis* methanolic extract, (B): synthesized (CAgNPs) methanolic extract

Fourier transformation infrared spectroscopy (FTIR)

Fourier transformation infrared spectroscopy (FTIR) analysis was employed to identify functional groups that may be responsible for the reduction/ bio-reduction of AgNO_3 to Ag-NPs and their stabilization. FTIR spectroscopy is a technique used to measure the vibration frequencies of the bonds in molecules. It is used to confirm the presence of the functional groups of the active components in the synthesized AgNPs based on the band value in the region of the infrared radiation³³. The dual role of the plant extract as a bio-reduction and capping agent was confirmed by FTIR analysis of the prepared AgNPs of *Camellia sinensis* leaves extract.

Fourier Transform Infra-Red (FTIR) spectrophotometers were used for recording spectra in the region 4000 cm^{-1} to 670 cm^{-1} ($2.5\text{ }\mu\text{m}$ to $15\text{ }\mu\text{m}$) or in some cases down to 200 cm^{-1} ($50\text{ }\mu\text{m}$). The results of the FTIR Spectra of the *Camellia sinensis* methanolic and aqueous extracts revealed the presence of different functional groups such as Phenolic–OH group stretching, C-H stretching, N-H bend, C-C stretching and C-N stretching, and had

prominent bands of absorbance at peaks (3394.72 , 2935.66 , 1627.92 , 1443.82 , and 1018.41) cm^{-1} for methanolic extract and (3417.86 , 2939.52 , 1637.56 , 1448.54 , and 1041.56) cm^{-1} for aqueous extract respectively (Table 1). Moreover, the FTIR spectroscopy showed that samples analysis had prominent bands of absorbance at peaks (3421.72 , 2937.59 , 2358.94 , 1643.35 , 1369.46 and 1037.70) cm^{-1} for aqueous (CAgNPs) extract, and the absorption bands appeared at (3433.29 , 1649.14 , 1373.32 and 1029.99) cm^{-1} for the methanolic (CAgNPs) extract Figs. 3 and 4.

The presence of a functional group in the synthesized AgNPs was similar to that reported by Waris *et al.*³⁴ where the FTIR spectrum showed the carbonyl group formed amino acid residues and this finding is in agreement with other researchers^{13,35} who also found that proteins have stronger affinity for binding metal, suggesting that the proteins may form metal nanoparticles (i.e., cap silver nanoparticles) to prevent agglom. Das *et al.*³⁶ mentioned the changes in the functional groups in active biomolecules might suggest their involvement in the synthesized of (AgNPs).

Table 1. IR frequencies region for the functional groups of the *Camellia sinensis* leaves extracts

The Functional Group	I.R wave number Standard groups	I.R wave number methanolic extract	I.R wave number aqueous extract	I.R wave number methanolic CAgNPs extract	I.R wave number aqueous CAgNPs extract
Phenolic groups stretching	3650-2500	3394.72	3417.86	3433.29	3421.72
C-H stretching	2960-2850	2935.66	2939.52	-----	2937.59
N-H band	1650-1580	1627.92	1637.56	1649.14	1643.35
C-C stretching	1500-1400	1443.82	1448.54	-----	-----
C-N stretching	1250-1020	1018.41	1041.56	1029.99	1037.70

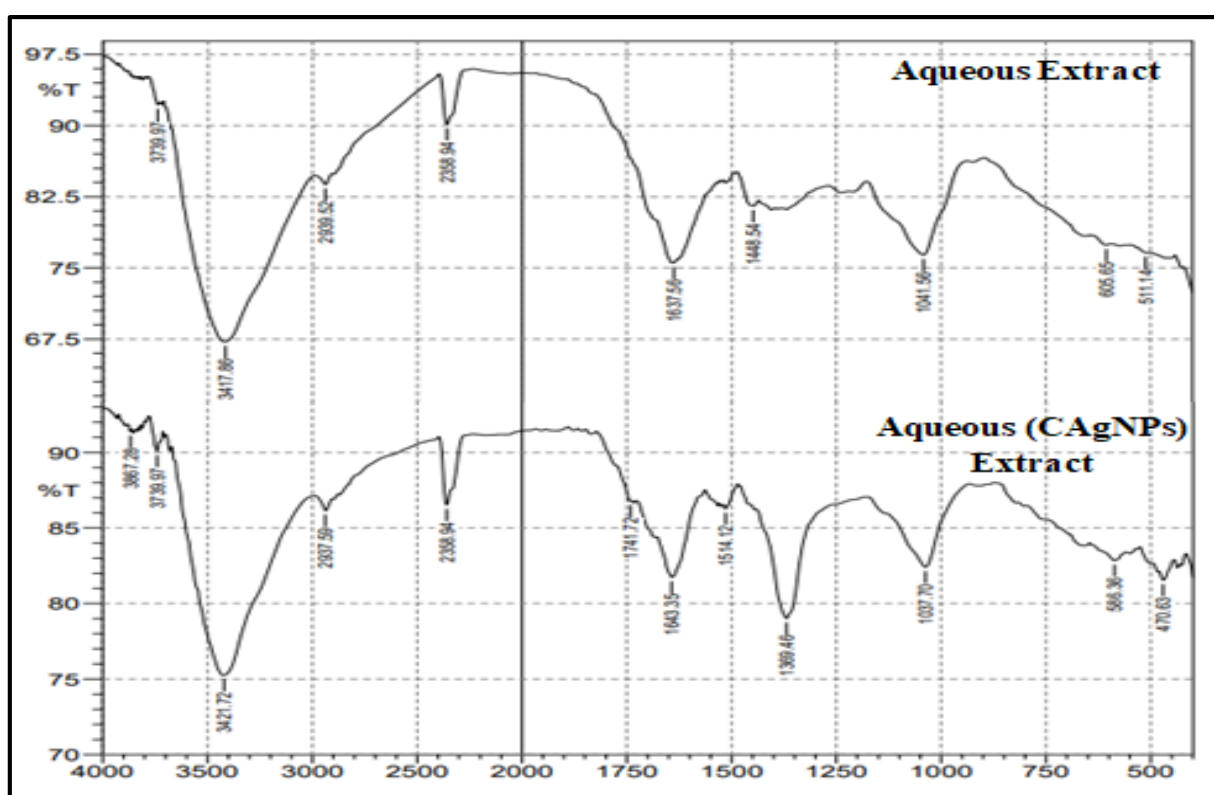


Figure 3. FTIR Spectra Pattern of *Camellia sinensis* aqueous extract and (CAgNPs) aqueous extract

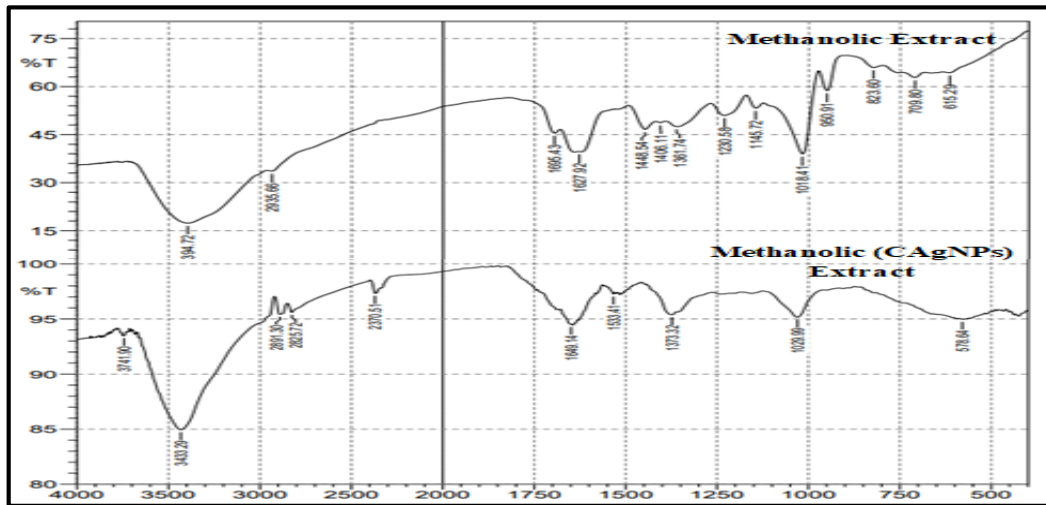


Figure 4. FTIR Spectra Pattern of *Camellia sinensis* methanolic extract and (CAgNPs) methanolic extract

Atomic force microscopy (AFM)

The CAgNPs aqueous and methanolic extracts were spherical in form, either singly or in aggregates, according to the results of the AFM study, in both the two-dimensional and three-dimensional views. The average particle size for the two types of extracts was also revealed by the AFM investigation was 108.3 nm and 84.76 nm, for CAgNPs aqueous and methanolic extract respectively Figs. 5 and 6. The finding was in agreement with Silver nanoparticles

that were produced by biosynthesis were virtually spherical, solitary 25–50 nm, or found in clumps 100 nm, according to Bhat *et al.*³⁷. According to Githala *et al.*³⁸ who used an atomic force microscope to measure the size and shape of partials, silver particles had an irregular polygonal form and had diameters ranging from 1.0 to 130 nm. The average nanoparticulate dimension was 63.3 nm. While the particles of Ag and ZnO were irregular, LiO2 appeared elongated and irregular, even though their diameters varied from 1.8 to 2.24 nm, respectively³⁹.

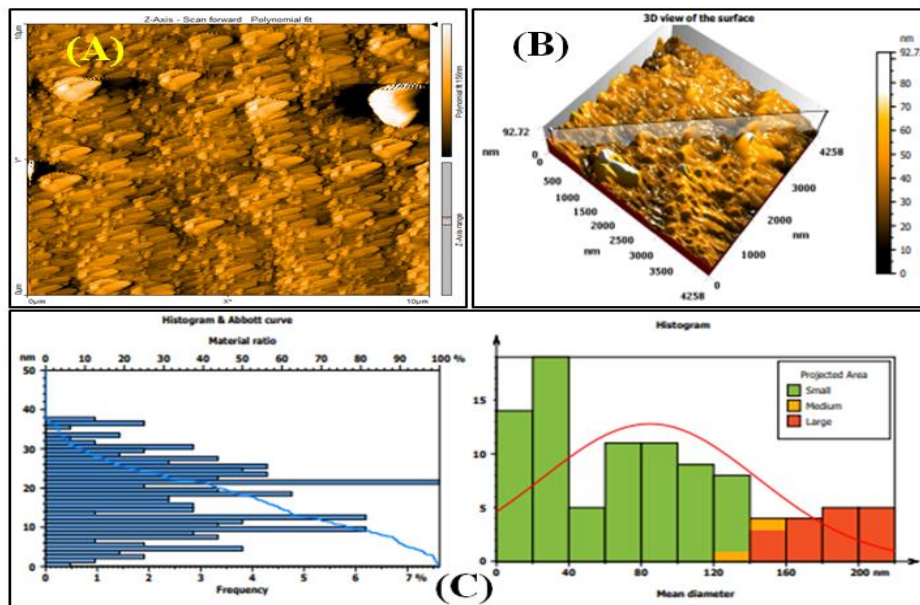


Figure 5. Atomic force microscopy analysis of CAgNPs methanolic extract (A): Two-dimensional of CAgNPs methanolic extract, (B): Three-dimensional of CAgNPs methanolic extract, (C): AFM diagram of size range of CAgNPs methanolic extract.

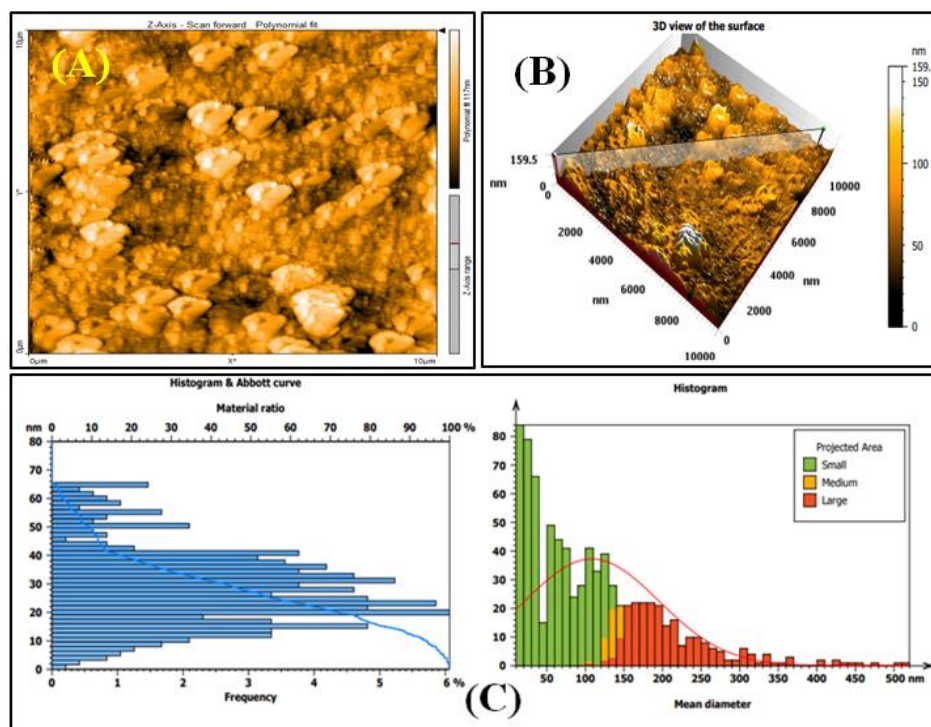


Figure 6. Atomic force microscopy analysis of CAgNPs aqueous extract (A): Two-dimensional of CAgNPs aqueous extract, (B): Three-dimensional of CAgNPs methanolic extract, (C): AFM diagram of size range of CAgNPs aqueous extract.

X-ray diffractometer

An effective method for assessing crystalline materials is the X-ray diffractometer (XRD), which offers data on structures, phases, preferred crystal orientations, and other structural characteristics including average grain size, crystallinity, strain, and crystal defects⁴⁰.

AgNPs were produced sustainably thanks to X-ray diffraction (XRD). For the CAgNPs methanolic extract, diffraction peaks were clearly visible at 2θ values 38.229, 44.349, 64.580, and 77.464, which corresponded to 111, 200, 220, and 311 planes of silver, respectively as shown in Fig. 7. For the CAgNPs aqueous extract, diffraction peaks were visible at 2θ values 38.175, 44.325, 64.543, and 77.472, corresponded to 111, 200, 220 and 311 planes of silver respectively as shown in Fig. 8.

By reducing Ag⁺ ions with *Camellia sinensis* extracts, AgNPs were generated, as was evident from the XRD pattern found in crystals. Some unassigned peaks were found, which may have been caused by the bio-organic phase metalloproteins that were

present on the surface of the silver nanoparticles or by the plant extracts lower concentration of biomolecules that function as stabilizing agents like enzymes or proteins¹².

The average crystallite sizes according to Debye–Scherrer equation calculated are found to be 99.66 and 61.24 nm for CAgNPs methanolic and aqueous extracts respectively. The finding agrees with the study by Ssekatawa *et al.*¹² used an aqueous extract of *Camellia sinensis* bark to create silver nanoparticles, silver nanoparticles have shown clear peaks of cubic phases at 38.0 (111), 44.3 (200), 64.5 (220) and 77.4 (311). And Rakaa and Obaid⁴¹ were involved a synthesis of silver nanoparticle using of Thyme Leaf Extracts bark, silver nanoparticles have shown clear peaks of cubic the peaks at 2θ of 38.45°, 44.39°, 64.57°, and 77.54° are corresponding to the crystallographic planes 111, 200, 220 and 311, respectively.

Interestingly, most of the researchers^{34, 40, 42, 43} that synthesized the nanoparticles using plant extracts seem to obtain a similar crystal structure. Whereas several reports state that the NPs produced

by reacting AgNO_3 with biological solutions are face-centered cubic with slight variations in peak values based on the kind of extract, metabolites present, and binding characteristics ⁴⁴.

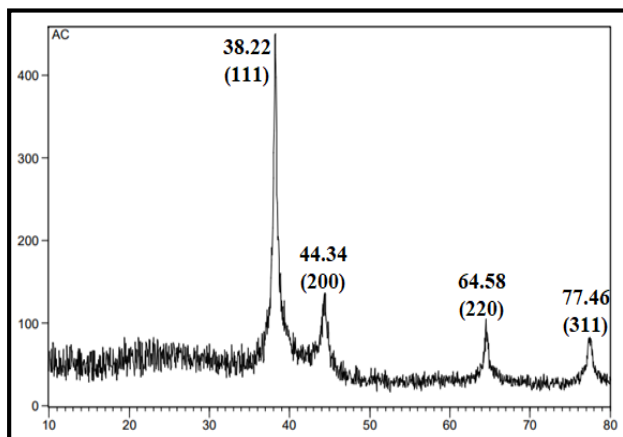


Figure 7. The XRD pattern of CAgNPs methanolic extract

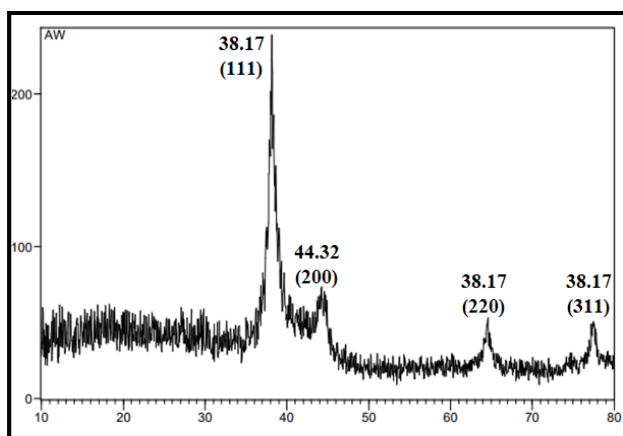


Figure 8. The XRD pattern of CAgNPs aqueous extract

Analysis of the zeta potential

The results of the synthesized molecules' nanoparticles' zeta potential values were -30.31 and -32.33 mV for CAgNPs aqueous and methanolic extracts respectively, Fig. 9 and 10.

The stability of colloidal dispersions is largely determined by the zeta analysis. A measure of how strongly neighboring similarly charged particles are attracted to one another electrostatically in dispersion is expressed by the magnitude of the zeta potential. A strong zeta potential will confer stability to sufficiently small molecules and particles, implying that the solution or dispersion will resist

aggregation. Colloids with high zeta potentials (positive or negative) are electrically stable, but those with low zeta potentials coagulate or flocculate because the dispersion might shatter and flocculate if attractive forces outweigh the repulsion ⁴⁵. In general, the nanoparticles' zeta potential should be more than +30 mV or less than -30 mV ⁴⁶.

The finding agrees with Surega ⁴⁷, who discovered that the zeta analysis of green produced AgNPs was -41.7, -27.9, and -37.2 mV using plant extracts of *Tridax procumbens*, *Euphorbia hirta*, and *Azardirachta indica*, respectively. The Zeta potential distributed with wide range of -41.7 mV indicated the highly stable nature of AgNPs synthesized using *T. procumbens* extract. Anandalakshmi and Venugobal ⁴⁸ synthesized AgNPs using *Vitex negundo* leaf extract, zeta potential value was -13.5mV which was incipient instability.

Many of the physiologically active substances included in natural extracts may be to blame for both the stability of the generated nanoparticles and the drop in silver ions. By transforming silver ions into AgNPs, phytochemicals such as phenolics, coumarins, terpenoids, glycosides, alkaloids, and tannins may function as bio reductants in this green synthesis technique. Furthermore, it's possible that the peptides and proteins in turmeric and cinnamon extracts will aid in the production of silver nanoparticles and will lessen the number of silver ions in silver ⁴⁹.

Additionally, because proteins' carbonyl groups have a strong affinity for bonding to metal nanoparticles, they can deposit a coating layer on the surface of AgNPs. As a result, the generated nanoparticles are less likely to aggregate and are more stable in aquatic environments ⁵⁰.

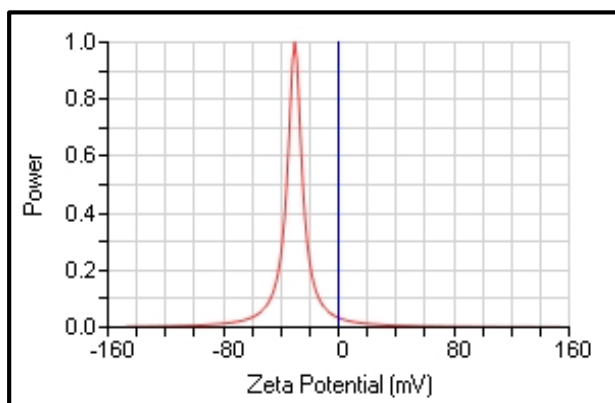


Figure 9. The zeta potential value of CAgNPs aqueous extract.

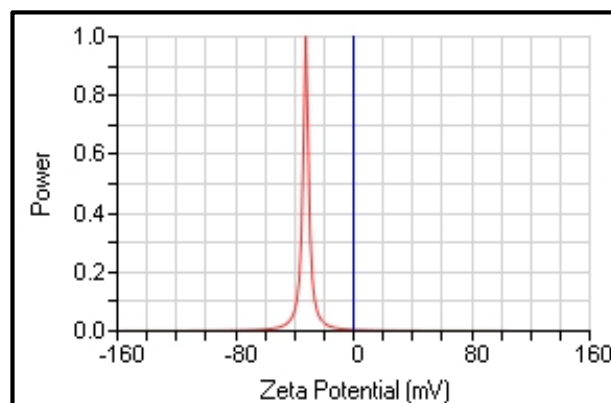


Figure 10. The zeta potential value of CAgNPs methanolic extract.

Conclusion

This study concluded that the aqueous and methanolic extracts of *Camellia sinensis* leaves contain phenolic compounds and the presence of a variety of active compounds in addition to the safe

handling and low costs of this can be used as a good reductant for the non-toxic or green synthesis of metallic silver nanoparticles.

Authors' Declaration

- Conflicts of Interest: None.
- I hereby confirm that all the Figures and Tables in the manuscript are mine. Furthermore, any Figures and images, that are not mine, have been

- included with the necessary permission for republication, which is attached to the manuscript.
- Ethical Clearance: The project was approved by the local ethical committee in University of Baghdad.

References

1. Hossain MI, Soliman MM, El-Naggar ME, Sultan MZ, Kechi A, Abdelsalam NR Chowdhury M. Synthesis and characterization of graphene oxide-ammonium ferric sulfate composite for the removal of dyes from tannery wastewater. *J Mater Res Technol. Tec.* 2021 May 1; 12: 1715-27. <https://doi.org/10.1016/J.JMRT.2021.03.097>.
2. Al Saqr A, Khafagy ES, Alalawi A, Aldawsari MF, Alshahrani SM, Anwer MK, et al. Synthesis of gold nanoparticles by using green machinery: Characterization and in vitro toxicity. *J Nanomater.* 2021; 11(3): 808. <https://doi.org/10.3390/nano11030808>.
3. Rónavári A, Igaz N, Adamecz DI, Szerencsés B, Molnar C, Kónya Z, et al. Green silver and gold nanoparticles: Biological synthesis approaches and potentials for biomedical applications. *Molecules.* 2021; 26(4): 844. <https://doi.org/10.3390/molecules26040844>.
4. Mosa WF, Ali HM, Abdelsalam NR. The utilization of tryptophan and glycine amino acids as safe alternatives to chemical fertilizers in apple orchards. *Environ. Sci Pollut Res.* 2021; 28(2): 1983-91. <https://doi.org/10.1007/s11356-020-10658-7>.
5. Yang Y, Jin P, Zhang X, Ravichandran N, Ying H, Yu C, et al. New epigallocatechin gallate (EGCG) nanocomplexes co-assembled with 3-mercapto-1-hexanol and β lactoglobulin for improvement of antitumor activity. *J Biomed Nanotechnol.* 2017; 13: 805–14. <https://doi.org/10.1166/jbn.2017.2400>.
6. Corciova A, Ivanescu B. Biosynthesis, characterisation and therapeutic applications of plant-mediated silver nanoparticles. *J Serb Chem Soc.* 2018; 83(5): 515-38. <https://doi.org/10.2298/JSC170731021C>.
7. Qurat U, Raja AQ, Sarfraz A. Mechanism of Action of bio-inspired nanosilver particles. *Bioinspired Biomim Nanobiomaterials.* 2018; 7(3): 174-86. <https://doi.org/10.1680/jbibn.17.00026>
8. Deepika S, Selvaraj CI, Roopan SM. Screening bioactivities of *Caesalpinia pulcherrima* L. swartz and cytotoxicity of extract synthesized silver nanoparticles on HCT116 cell line. *Mater Sci Eng.* 2020; 106: 110279. <https://doi.org/10.1016/j.msec.2019.110279>.

9. Srivastava S, Usmani Z, Atanasov AG, Singh VK, Singh NP, Abdel-Azeem AM, et al. Biological nanofactories: Using living forms for metal nanoparticle synthesis. *Mini-Rev Med Chem.* 2021; 21(2): 245-65. <https://doi.org/10.2174/1389557520999201116163012>.
10. Şimşek B, Sevgili İ, Ceran ÖB, Korucu H. Tools and Techniques for Purification of Water Using Nano Materials. *Health and Safety.* Springer, Berlin, Heidelberg. 2019 ; 22; (pp. 285-322).
11. Dosoky WM, Fouda MM, Alwan AB, Abdelsalam NR, Taha AE, Ghareeb RY, et al. Dietary supplementation of silver-silica nanoparticles promotes histological, immunological, ultrastructural, and performance parameters of broiler chickens. *Sci Rep.* 2021; 11(1): 1-15. <https://doi.org/10.1038/s41598-021-83753-5>.
12. Ssekatawa K, Byarugaba D, Kato C, Nakavuma J, Wampande E, Ejobi F, et al. Physiochemical properties and antibacterial activity of silver nanoparticles green synthesized by *Camellia sinensis* and *Prunus africana* extracts. *Res sq* 2021; 21. DOI: <https://doi.org/10.21203/rs.3.rs-143995/v1>.
13. Ojha S, Sett A, Bora U. Green synthesis of silver nanoparticles by *Ricinus communis* var. *carmencita* leaf extract and its antibacterial study. *Adv Nat Sci : Nanosci Nanotechnol.* 2017; 8(3): 35-39. <https://doi.org/10.1088/2043-6254/aa724b>.
14. Krishnadhas L, Santhi R, Annapurani S. Green Synthesis of Silver Nanoparticles from the Leaf Extract of *Volkameria inermis*. *Int J Pharm Clin Res.* 2017; 9(8): 610-16. <https://doi.org/10.25258/ijpcr.v9i08.9587>.
15. Elbossaty WF. Green tea as biological system for the synthesis of silver nanoparticles. *J biotechnol biomater.* 2017; 7(269). <https://doi.org/10.4172/2155-952X.1000269>
16. Ashraf A, Zafar S, Zahid K, Salahuddin M, Al-Ghanim KA, Al-Misned F. Synthesis, characterization, and antibacterial potential of silver nanoparticles synthesized from *Coriandrum sativum* L. *J Infect Public Health.* 2019; 12(2): 275-81. <https://doi.org/10.1016/j.jiph.2018.11.002>, PMID 30477919.
17. Chaudhuri SK, Chandela S, Malodial L. Plant Mediated Green Synthesis of Silver Nanoparticles Using *Tecomella undulata* Leaf Extract and Their Characterization. *Nano Biomed Eng.* 2016; 8(1): 1-8. <https://doi.org/10.5101/nbe.v8i1.p1-8>.
18. Hammodi H.F, Rashid IH, Oraibi AG. “Green biosynthesis, Identification and characterization of Ag and Zn nanoparticles using Ivy (*Epipremnum aureum*) plant extract,” *Plant Arch.* 2019; 19(2): 959–65. <https://doi.org/10.1016/j.kijoms.2017.10.007>.
19. Lakshmanan G, Kalaichelvan SA, Murugesan K. Plant-mediated synthesis of silver nanoparticles using fruit extract of *Cleome viscosa* L.: Assessment of their antibacterial and anticancer activity. *Karbala Int J Mod Sci.* 2018; 4(1): 61-8. <https://doi.org/10.3390/nano8030174>.
20. Aljabali AA, Akkam Y, Al-Zoubi MS, Al-Batayneh KM, AlTrad B, Abo Alrob O, et al. Synthesis of Gold Nanoparticles Using Leaf Extract of *Ziziphus zizyphus* and their Antimicrobial Activity. *J Nanomater.* 2018; 8(3): 174-88. <https://doi.org/10.3109/21691401.2016.1160403>.
21. Arokiyaraj S, Vincent S, Saravanan M, Lee Y, Oh YK, Kim KH. Green synthesis of silver nanoparticles using *Rheum palmatum* root extract and their antibacterial activity against *Staphylococcus aureus* and *Pseudomonas aeruginosa*. *Artif Cells Nanomed Biotechnol.* 2017; 45: 372–79. <https://doi.org/10.15739/ibspr.18.005>.
22. Obiazikwor OH, Shittu HO. Antifungal activity of silver nanoparticles synthesized using *Citrus sinensis* peel extract against fungal phytopathogens isolated from diseased tomato (*Solanum lycopersicum* L.). *Issues Biol. Sci Pharm Res.* 2018; 6(3): 30-38. <https://doi.org/10.15739/ibspr.18.005>
23. Salleh A, Naomi R, Utami ND, Mohammad AW, Mahmoudi E, Mustafa N. The potential of silver nanoparticles for antiviral and antibacterial applications: A mechanism of action. *J Nanomater.* 2020; 10(1566): 20. <https://doi.org/10.3390/nano10081566>.
24. Saliem AH, Ibrahim OM, Salih SI. Biosynthesis of Silver Nanoparticles using *Cinnamon zeylanicum* Plants Bark Extract. *Kufa j vet Sci.* 2016; 7(1): 51- 63. <https://doi.org/10.1155/2022/4894642>.
25. Oraibi AG, Yahia HN, Alobaidi KH. Green Biosynthesis of Silver Nanoparticles Using *Malva parviflora* Extract for Improving a New Nutrition Formula of a Hydroponic System. *Hindawi Scientifica.* 2022 May 30. Article ID 4894642, 10 pages. <https://doi.org/10.1155/2022/4894642>
26. Femi-Adepoju AG, Dada AO, Otun KO, Adepoju AO, Fatoba OP. Green synthesis of silver nanoparticles using terrestrial fern (*Gleichenia Pectinata* (Willd.) C. Presl.): characterization and antimicrobial studies. *Heliyon.* 2019; 5(4): e01543. <https://doi.org/10.1016/j.heliyon.2019.e01543>
27. Mohamed, H. E. A., Afridi, S., Khalil, A. T., Zia, D., Iqbal, J., Ullah, I., ... & Maaza, M. (2019). Biosynthesis of silver nanoparticles from *Hyphaene*

- thebaica fruits and their in vitro pharmacognostic potential. *Materials Research Express*, 6(10), 1050c9. <https://doi.org/10.1088/2053-1591/ab4217>.
28. Asimuddin M, Shaik MR, Adil SF, Siddiqui MRH, Alwarthan A, Jamil K, et al. Azadirachta indica based biosynthesis of silver nanoparticles and evaluation of their antibacterial and cytotoxic effects. *J King Saud Univ Sci*. 2020; 32(1): 648-656. <https://doi.org/10.1016/j.jksus.2018.09.014>
29. Mohamed HEA, Afridi S, Khalil AT, Zia D, Iqbal J, Ullah I, et al. Biosynthesis of silver nanoparticles from *Hyphaene thebaica* fruits and their in vitro pharmacognostic potential. *Mater. Res Express*. 2019; 6(10): 1050c9. <https://doi.org/10.1088/2053-1591/ab4217>.
30. Venugopal K, Rather HA, Rajagopal K, Shanthi MP, Sheriff K, Illiyas M, et al. Synthesis of silver nanoparticles (Ag NPs) for anticancer activities (MCF 7 breast and A549 lung cell lines) of the crude extract of *Syzygium aromaticum*. *J Photochem. Photobiol B, Biol*. 2017; 167: 282-89. <https://doi.org/10.1016/j.jphotobiol.2016.12.013>.
31. Mohammad DAE, Al-Jubouri SHK. Comparative antimicrobial activity of silver nanoparticles synthesized by *Corynebacterium glutamicum* and plant extracts. *Baghdad Sci J*. 2019; 16(3 Suppl.): 689-696. [https://dx.doi.org/10.21123/bsj.2019.16.3\(Suppl.\).0689](https://dx.doi.org/10.21123/bsj.2019.16.3(Suppl.).0689).
32. Zhang XF, Liu ZG, Shen W, Gurunathan S. Silver nanoparticles: synthesis, characterization, properties, applications, and therapeutic approaches. *Int J Mol Sci*. 2016; 17(9):1534. <https://doi.org/10.3390/ijms17091534>.
33. Saad AM, El-Saadony MT, El-Tahan AM, Sayed S, Moustafa MAM, Taha AE. Polyphenolic extracts from pomegranate and watermelon wastes as substrate to fabricate sustainable silver nanoparticles with larvicidal effect against *Spodoptera littoralis*. *Saudi J Biol Sci*. 2021; 28 (10): 5674-83. [https://doi.org/10.1016/j.sjbs.\(2021\).06.011](https://doi.org/10.1016/j.sjbs.(2021).06.011), PMID 34588879.
34. Waris M, Nasir S, Rasule A, Yousaf I. Evaluation of larvicidal efficacy of *Ricinus communis* (Castor) plant extract and synthesized green silver nanoparticles against *Aedes albopictus*. *J Arthropod-Borne Dis*. 2020; 14(2): 162-72. <https://doi.org/10.18502/jad.v14i2.3734>.
35. Moteriya P, Chanda S. Biosynthesis of silver nanoparticles formation from *Caesalpinia pulchella* stem metabolites and their broad spectrum biological activities. *J Genet Eng Biotechnol*. 2018; 16: 105-13. <https://doi.org/10.1016/j.jgeb.2017.12.003>.
36. Das G, Patra JK, Nagaraj CNV, Shin HS. Comparative study on antidiabetic, cytotoxicity, antioxidant and antibacterial properties of biosynthesized silver nanoparticles using outer peels of two varieties of *Ipomoea batatas* (L.) Lam. *Int J Nanomedicine*. 2019; 14: 4741. <https://doi.org/10.2147/IJN.S210517>.
37. Bhat M, Chakraborty B, Kumar RS, Almansour AI, Arumugam N, Kotresha D, et al. Biogenic synthesis, characterization and antimicrobial activity of *Ixora brachypoda* (DC) leaf extract mediated silver nanoparticles. *J King Saud Univ Sci*.2021; 33(2): 101296. <https://doi.org/10.1016/j.jksus.2020.101296>.
38. Githala CK, Raj S, Dhaka A, Mali SC, Trivedi R. Phyto-fabrication of silver nanoparticles and their catalytic dye degradation and antifungal efficacy. *Front Chem*. 2022; 10. <https://doi.org/10.3389/fchem>.
39. Auda, M. M., Shareef, H. A., & Mohammed, B. L. (2021). Green synthesis of Silver Nanoparticles using the extract of *Rheum ribes* and evaluating their antifungal activity against some of *Candida* sp. *Tikrit Journal of Pure Science*, 26(2), 53-59. <https://doi.org/10.25130/tjps.v26i2.119>.
40. Salari S, Bahabadi SE, Samzadeh-Kermani A, Yosefzai F. In-vitro evaluation of antioxidant and antibacterial potential of green synthesized silver nanoparticles using *Prosopis farcta* fruit extract. *Iran J Pharm Res*. 2019; 18(1): 430-455.
41. Rakaa JM, Obaid AS. Preparation of Nanoparticles in an Eco-friendly Method using Thyme Leaf Extracts. *Baghdad Sci J*. 2020; ;17(2(SI):0670. <http://dx.doi.org/10.21123/bsj>.
42. Xu M, Liu J, Xu X, Liu S, Peterka F, Ren Y. Synthesis and comparative biological properties of Ag-PEG nanoparticles with tunable morphologies from janus to multicore shell structure. *Materials*. 2018; 11(10): 1787. <https://doi.org/10.3390/ma11101787>.
43. Faraj MM, ad AL-Jobor KM. Green synthesis of silver nanoparticles using tomato (*Lycopersicon esculentum*) extracts and evaluation of their antifungal activity. *Plant Arch*. 2020; 20 (2): 5777-5786.
44. Ghramh HA, Khan KA, Ibrahim EH, Setzer WN. Synthesis of gold nanoparticles (AuNPs) using *Ricinus communis* leaf ethanol extract, their characterization, and biological applications. *J Nanomater*. 2019; 9: 765. <https://doi.org/10.3390/nano9050765>.
45. González-Ballesteros N, Prado-López S, Rodríguez-González JB, Lastra M, Rodríguez-Argüelles MC. Green synthesis of gold nanoparticles using brown algae *Cystoseira baccata*: Its activity in colon cancer cells. *Colloids Surf B*. 2017; 153: 190-98. <https://doi.org/10.1016/j.colsurfb.2017.02.020>.
46. Elamawi RM, Al-Harbi RE, Hendi AA. Biosynthesis and characterization of silver nanoparticles using

- Trichoderma longibrachiatum and their effect on phytopathogenic fungi. Egypt J Biol Pest Control. 2018; 28:1-11. <https://doi.org/10.1186/s41938-018-0028-1>.
47. Al-Khafaji A R, Al-Azawi A H. Green Method Synthesis of Silver Nanoparticles Using Leaves Extracts of Rosmarinus officinalis. Iraqi J Biotechnol. 2022; 21(2): 251-267.
48. Anandalakshmi K, Venugobal J. Green synthesis and characterization of silver nanoparticles using Vitex negundo (Karu Nochchi) Leaf Extract and its Antibacterial Activity. Med Chem (Los Angeles). 2017; 7(7): 218-25. <https://doi.org/10.4172/2161-0444.1000460>.
49. Dhand V, Soumya L, Bharadwaj S, Chakra S, Bhatt D, Sreedhar B. Green synthesis of silver nanoparticles using Coffea arabica seed extract and its antibacterial activity. Mater Sci Eng C. 2016; 58: 36-43. <https://doi.org/10.1016/j.msec.2015.08.018>.
50. Nikam SA, Chaudhari SP. Biosynthesis of Silver Nanoparticles from Polyphenolic Extract of Baliospermum solanifolium using Central Composite Design. Pharm Res. 2022; 14(4): 405-11. <https://doi.org/10.5530/pres.14.4.59>.

التخليق الحيوي لجسيمات الفضة النانوية باستخدام مستخلصات الشاي الأخضر

هوازن صالح

قسم الهندسة الوراثية، معهد الهندسة الوراثية والتقنيات الاحيائية للدراسات العليا، جامعة بغداد، بغداد، العراق.

الخلاصة

اصبح تركيب جسيمات الفضة النانوية بالطرق الخضراء بواسطة النباتات شائعًا بشكل متزايد بسبب ملاءمته للبيئة، وتوفره، وفعالته وكلفته القليلة، ويمكن التعامل معه بأمان ويمتلك تنوعًا واسعًا من المركبات الفعالة، مثل مضادات الأكسدة و مركبات مضادة للميكروبات. في الدراسة الحالية، تم تصنيع جسيمات الفضة النانوية AgNPs باستخدام المستخلصات المائية والميثانولية لأوراق الشاي الاخضر التي اختزلت نترات الفضة، والتي تم توصيفها باستخدام العديد من التقنيات التحليلية مثل القياس الطيفي المرئي فوق البنفسجي (UV-Vis)، والتحويل الطيفي بالأشعة تحت الحمراء (FTIR)، والفحص المجهرى الذري (AFM)، وتشتت الأشعة السينية (XRD) وفحص جهد زيتا. أشارت الملاحظة البصرية إلى أن لون نترات الفضة المائية قد تحول بعد المعاملة بمستخلصات الأوراق وتؤكد ذلك بواسطة أطياف UV-Vis. فضلا عن ذلك، أظهر تحليل AFM أن الجسيمات كانت كروية الشكل، مفردة أو في مجاميع بمتوسط أحجام 108.3 و 84.76 نانومتر للمستخلصات المائية والميثانولية على التوالي. كذلك، أكدت تقنية XRD الطبيعة البلورية للجسيمات النانوية. وتم تقدير متوسط الحجم وفقاً لمعادلة شيرير اذ بلغت 61.24 و 99.66 نانومتر للمستخلصات المائية والميثانولية (CANPs) على التوالي. بالإضافة إلى قيم زيتا المحتملة كانت -30.31 و -32.33 مللي فولت للمستخلصات المائية والميثانولية CANPs على التوالي.

الكلمات المفتاحية: الاشعة البنفسجية، الاشعة تحت الحمراء، الاشعة السينية، الشاي الاخضر، المجهر الذري، تشتت جهد زيتا، جسيمات الفضة النانوية.